

A microstrip tunable negative refractive index metamaterial and phase shifter

P. He,^{1,a)} J. Gao,¹ C. T. Marinis,¹ P. V. Parimi,^{1,2} C. Vittoria,¹ and V. G. Harris¹

¹Center for Microwave Magnetic Materials and Integrated Circuits, Department of Electrical and Computer Engineering, Northeastern University, Boston, Massachusetts 02115, USA

²Department of Physics, Northeastern University, Boston, Massachusetts 02115, USA

(Received 4 June 2008; accepted 20 October 2008; published online 11 November 2008)

A tunable negative refractive index metamaterial and miniature phase shifter have been designed and fabricated in a microstrip configuration for applications in radio frequency integrated circuits. The metamaterial consists of plasmonic copper wires and yttrium iron garnet slabs having a low insertion loss of 5 dB at the center of the transmission band. The yttrium iron garnet material enables the magnetic field tuning of the negative refractive index in a dynamic frequency band from 7.0 to 11.0 GHz. The insertion phase can be tuned by 45° continuously by varying the bias field from 3.8 to 4.6 kOe at 9.0 GHz. © 2008 American Institute of Physics. [DOI: 10.1063/1.3025303]

The growth in rf and wireless mobile devices that operate at microwave frequencies has resulted in considerable demands for advanced materials and integrated circuits capable of operating at such frequencies in order to accomplish functions such as phase shift, frequency division, attenuation, isolation, and circulation for antennas. GaAs and silicon-based integrated circuit (IC) technologies have been commonly used in radio frequency ICs (RFICs) for telecommunication and sensor systems.¹ Silicon-based digital and analog microelectromechanical system phase shifters have been designed for beam steering phased array antenna systems² and recently attempts have been made to design superconducting phase shifting elements.³ Demands for size reduction and performance improvement in microwave links, phased arrays, radars, and remote sensing applications call for the development of advanced materials and miniature devices.

Recently developed artificial negative refractive index metamaterials (NIMs) have made available innovative rf device designs by taking advantage of the unique left-handed electromagnetic properties of these materials.^{4–13} However, the widely adopted metallic split ring resonator (SRR) based NIMs are limited by inherent narrow bandwidths and lack the ability to frequency tune essential properties. In order to obtain negative refractive index at various frequencies, one would have to change the periodicity and size of the elements. Alternatively, magnetic materials have been recently used to fabricate tunable NIMs (TNIMs)^{14–17} which possess negative refractive index bands tunable over wide frequency regions. In these designs, magnetic materials provide negative permeability at frequencies above their ferrimagnetic resonance (FMR). Notwithstanding their unique properties and frequency agile nature, these TNIMs were waveguide based and are incompatible with microwave integrated and printed circuit board designs.

A key aspect of the present research is the development of a planar microstrip TNIM that can form an integral part of TNIM-based RFIC devices such as a tunable phase shifter. In this letter, we report the design, fabrication, and test of a microstrip TNIM and phase shifter. Magnetic field tunable

passbands resulted from negative refractive index were realized in X-band (7–12.5 GHz). Both simulated and experimental data show tunable passbands resulting from negative refractive index. Although the reported TNIM composite has a minimum 5 dB insertion loss mainly due to impedance mismatch and magnetic loss, this work would enable further developments of TNIM-based RFIC devices, including planar transmission lines, coplanar waveguides, compact delay lines, circulators, phase shifters, and antennas.

As shown in the schematic of Fig. 1(a), the TNIM is composed of two alternate layers of periodic copper wires etched on laminated Kapton™ substrates and polycrystalline yttrium iron garnet (YIG) slabs. Polycrystalline YIG slabs (real part of relative permittivity, $\epsilon_r' = 15.0$), cut and polished from high density bulk material, were used. The linewidth of the YIG material, ΔH , is 50 Oe whereas the saturation magnetization, $4\pi M_s$, is 1750 G. Although polycrystalline YIG has higher absorption near its FMR than single crystal YIG due to a larger linewidth, it provides a wider frequency region between its FMR and antiferrimagnetic resonance (AFMR) where the permeability remains negative. This feature helps achieve a broader NIM passband. Periodic copper wires on Kapton™ ($\epsilon_r' = 3.9$) were prepared by wet etching

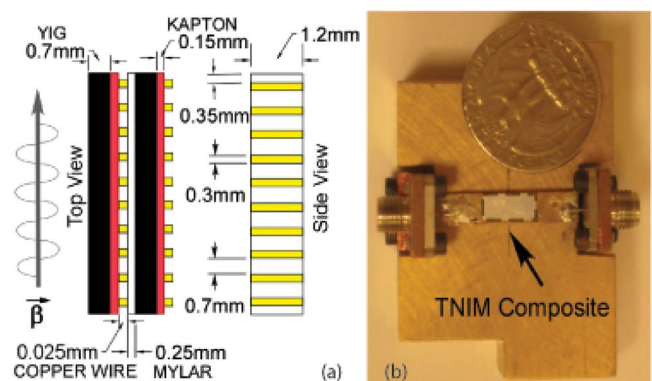


FIG. 1. (Color online) (a) Schematic top and side views of the $10.0 \times 2.0 \times 1.2 \text{ mm}^3$ TNIM composite. (b) Photograph of the microstrip test fixture, a $5 \times 25 \text{ mm}^2$ upper strip on the brass ground base relative to a U.S. quarter provided for a visual size comparison. The TNIM composite is mounted under the center of the upper strip.

^{a)}Electronic mail: he.pe@neu.edu.

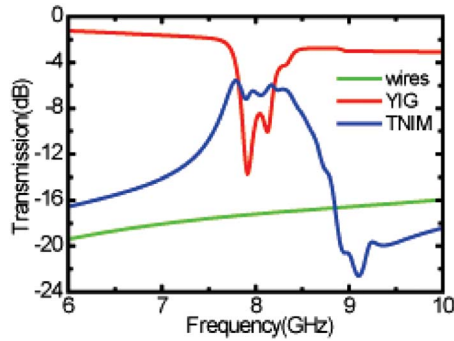


FIG. 2. (Color online) Simulated transmissions of the TNIM composite (blue circle), YIG slabs (red line), and Cu wires (green line). The magnetic bias field applied to the TNIM composite and YIG slabs is 3.5 kOe.

lithography using Dupont copper clad Kapton™ sheets. Mylar™ ($\epsilon_r' = 3.2$) spacers were cut from large sheets. The dielectric loss tangents of YIG, Kapton™, and Mylar are rather small and negligible in this design. All the components were glued together using Crazy Glue™.

The two Mylar™ pieces act as spacers between the wires and YIG slabs. The thicknesses of YIG slabs, Kapton™ substrates, and Mylar™ spacers are 0.70, 0.15, and 0.25 mm respectively. The copper wires have a length of 1.2 mm, a cross section of $0.025 \times 0.3 \text{ mm}^2$, and a center to center spacing of 1.0 mm. The height of the composite TNIM is 1.2 mm, which is also the vertical distance between the upper strip and the ground plane of the microstrip. The 10.0 mm long TNIM composite is mounted under the center of the upper strip with the rf electrical field and dc magnetic bias field along the long axis of the copper wires. In this assembly, the TNIM composite and air at the two ends act as substrates for the microstrip. Figure 1(b) is the photograph of the microstrip test fixture, the $5 \times 25 \text{ mm}^2$ brass upper strip on the ground base, positioned relative to a U.S. quarter to allow for size comparison.

In order to elucidate and demonstrate the validity of the TNIM design, the transmissions in the TNIM composite, YIG slabs, and copper wires are compared in finite element simulations using the Ansoft Inc. HFSS™ software suite as shown in Fig. 2. The applied magnetic bias field for the TNIM composite and YIG slabs is 3.5 kOe. Without the application of a magnetic bias field, the plasmonic effect of copper wires dominates, providing a negative permittivity so that there is no transmission below the plasma frequency (green line), which is designed to be much higher than 10 GHz. In the case of YIG slabs (red line), the dip in the region 7.7–8.4 GHz clearly indicates the FMR which results in negative permeability. Therefore, the broad transmission peak of the TNIM composite (blue line) is a result of negative refractive index.¹⁸ The dip near 9 GHz is attributed to the AFMR of the YIG material.¹⁹

A key advantage of the TNIM design is the magnetic field tunability of the passband over a wide range of frequency. In Fig. 3(a), the simulated transmissions of the TNIM composite under 3.0, 3.5, and 4.0 kOe show a clear frequency shift of the passband which is confirmed in measurements as shown in Fig. 3(b). As can be seen from Figs. 3(a) and 3(b), the simulated and measured results match very well validating the control achieved in the design on the TNIM and the dynamic bandwidth. The minimum insertion loss is around 5 dB. It is mainly due to the mag-

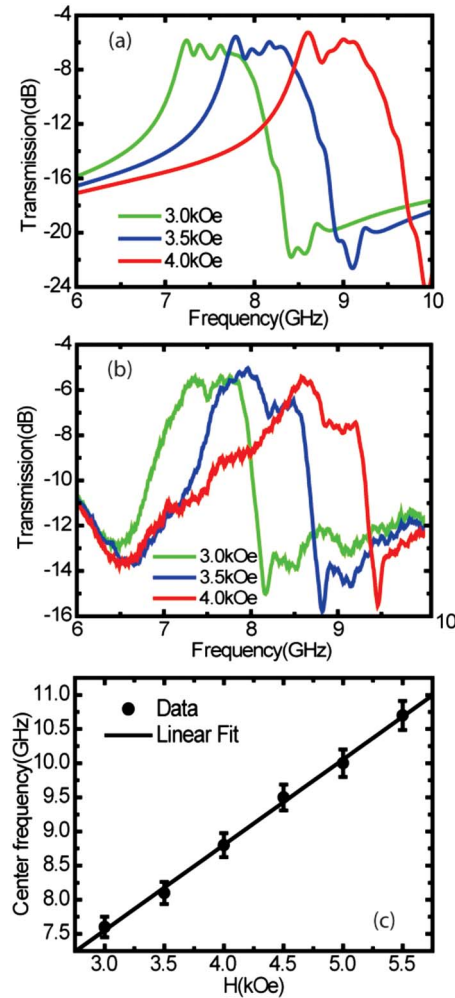


FIG. 3. (Color online) (a) Simulated and (b) measured 1.0 GHz wide TNIM passbands of over -8 dB transmission centered at 7.5, 8.0, and 8.8 GHz at magnetic bias fields of 3.0, 3.5, and 4.0 kOe, respectively. (c) Center frequency of the TNIM passband increases linearly from 7.6 to 10.7 GHz with the bias field changing from 3.0 to 5.5 kOe.

netic loss, eddy current loss, and impedance mismatch. The instantaneous bandwidth obtained is 1.0 GHz at a fixed bias field and the dynamic bandwidth is 2.3 GHz with a 1.0 kOe change in bias field. For comparison, the bandwidths of traditional SRR based NIM structures are generally smaller than 1.0 GHz.²⁰ In Fig. 3(c), the curve of the center frequency of TNIM passband versus the bias field is plotted. The center of TNIM passband is tuned linearly from 7.6 to 10.7 GHz by varying the bias field from 3.0 to 5.5 kOe, resulting in a tuning factor of 1.2 MHz/Oe.

One significant feature of the TNIM is the realization of transmission on the high frequency side of the FMR, where the permeability of the YIG materials is negative and changes rapidly. At a fixed frequency in this region, by varying the bias field, the TNIM composite would experience a rapid change in permeability which can generate a change in the refractive index, propagation constant, and insertion phase. Therefore, a magnetic field tunable phase shifter based on the TNIM can be realized. In Fig. 4, the experimental performance of the TNIM composite as a phase shifter at 9.0 GHz is presented. The field tuning of the insertion phase at 9.0 GHz shows a shift of 45° as the applied bias field varies from 3.94 to 4.58 kOe. The corresponding transmission in the TNIM varies from -6 to -10 dB as the result of

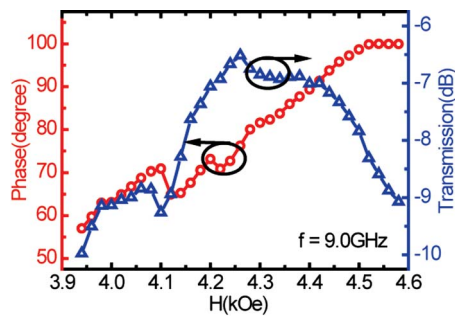


FIG. 4. (Color online) Measured phase shift and corresponding transmission vs the magnetic bias field of the TNIM composite at 9.0 GHz. The insertion phase shifts 45° while the transmission varies from -6 to -10 dB.

the change in wave impedance owing to the change in effective permeability. The tuning factor obtained is 70 deg/kOe .

In conclusion, we have constructed a wide band microstrip TNIM using copper wires and polycrystalline YIG slabs that operates in X-band. The 1.0 GHz wide instantaneous TNIM passband, having a peak transmission of -5 dB, is tunable between 7.6 and 10.7 GHz by changing the bias field from 3.0 to 5.5 kOe. The TNIM composite can perform as a tunable phase shifter where the insertion phase shifts 45° for a field change of 0.64 kOe. The $10.0 \times 2.0 \times 1.2 \text{ mm}^3$ TNIM composite is compact, mechanically robust, and compatible with planar microwave devices. Although the TNIM design still face the challenge of high insertion loss, this technology provides unique properties such as wide band and continuous frequency tunability of negative refractive index, which can enable designs and developments of innovative devices with enhanced functionality in small and lightweight constructs. Furthermore, using this device configuration on a multiferroic substrate has the potential to allow for electric field tunable phase shifters which are small, light, and operate beyond today's performance metrics. Such a device would enable real time beam steering of phased array radar among other RFIC applications.

The authors would gratefully acknowledge the colleagues Yajie Chen in the CM3IC and Zhuhua Cai in the Department of Chemical Engineering at Northeastern University for the beneficial discussions and suggestions. This research was supported by the Defense Advanced Research Program Agency, the National Science Foundation, and the Office of Naval Research.

- ¹T. M. Hancock and G. M. Rebeiz, *IEEE Trans. Microwave Theory Tech.* **53**, 977 (2005).
- ²N. Kingsley, P. Kirby, G. Ponchak, and J. Papapolymerou, Topical Meeting on Silicon Monolithic Integrated Circuits in RF Systems (unpublished) (2004).
- ³B. Dimov, D. Balashov, M. Khapipov, Th. Ortlepp, F.-Im. Buchholz, A. B. Zorin, J. Niemeyer, and F. H. Uhlmann, *Supercond. Sci. Technol.* **20**, 332 (2007).
- ⁴J. B. Pendry, *Phys. Rev. Lett.* **85**, 3966 (2000).
- ⁵R. A. Shelby, D. R. Smith, and S. Schultz, *Science* **292**, 77 (2001).
- ⁶P. V. Parimi, W. T. Lu, P. Vodo, J. Sokoloff, J. S. Derov, and S. Sridhar, *Phys. Rev. Lett.* **92**, 127401 (2004).
- ⁷C. M. Soukoulis, S. Linden, and M. Wegener, *Science* **305**, 1136481 (2007).
- ⁸A. Grbic and G. V. Eleftheriades, *J. Appl. Phys.* **98**, 043106 (2006).
- ⁹A. Sanada, C. Caloz, and T. Itoh, *IEEE Trans. Microwave Theory Tech.* **52**, 1252 (2004).
- ¹⁰G. Mumcu, K. Sertel, and J. L. Volakis, *IEEE Trans. Antennas Propag.* **5**, 168 (2006).
- ¹¹N. Engheta and R. W. Ziolkowski, *IEEE Trans. Microwave Theory Tech.* **53**, 1535 (2005).
- ¹²C. M. Krowne, *Phys. Rev. Lett.* **92**, 053901 (2004).
- ¹³L. Peng, L. Ran, H. Chen, H. Zhang, J. A. Kong, and T. M. Grzegorzczuk, *Phys. Rev. Lett.* **98**, 157403 (2007).
- ¹⁴Y. He, P. He, V. G. Harris, and C. Vittoria, *IEEE Trans. Magn.* **42**, 2852 (2006).
- ¹⁵Y. He, P. He, S. D. Yoon, P. V. Parimi, F. J. Rachford, V. G. Harris, and C. Vittoria, *J. Magn. Magn. Mater.* **313**, 187 (2007).
- ¹⁶P. He, P. V. Parimi, Y. He, V. G. Harris, and C. Vittoria, *Electron. Lett.* **43**, 1440 (2007).
- ¹⁷H. Zhao, J. Zhou, Q. Zhao, B. Li, and L. Kang, *Appl. Phys. Lett.* **91**, 131107 (2007).
- ¹⁸D. R. Smith, S. Schultz, P. Markos, and C. M. Soukoulis, *Phys. Rev. B* **65**, 195104 (2002).
- ¹⁹C. Vittoria, *Microwave Properties of Magnetic Films* (World Scientific, Singapore, 1993), pp. 107–112.
- ²⁰D. R. Smith, W. J. Padilla, D. C. Vier, S. C. Nemat-Nasser, and S. Schultz, *Phys. Rev. Lett.* **84**, 4184 (2000).